

## Controlled Assembly of Ultrasmall Iron Oxide Nanoparticles on Carbon Nanotubes: Facile Preparation and Interfacially Induced Ferromagnetism

Jiaoxing Xu, Ning Wang, and Lunhui Guan\*

State Key Structural Chemistry Laboratory, Fujian Institute of Research on the Structure of Matter, Chinese Academy of Sciences, Fujian 350002, P. R. China

(Received September 27, 2011; CL-110790; E-mail: guanlh@fjirsm.ac.cn)

Ultrasmall (<5 nm)  $\gamma$ -Fe<sub>2</sub>O<sub>3</sub> nanocrystals with tunable loading density on the carbon nanotubes (CNTs) were solvothermally synthesized using bifunctional phenol as capping ligand and dually as surfactant that favored uniform attachment. With the interfacial charge transfer, the nanosize-dependently superparamagnetic  $\gamma$ -Fe<sub>2</sub>O<sub>3</sub> nanoparticles transform to weak ferromagnetism at room temperature.

The attachment of nanoparticles (NPs) on carbon nanotubes (CNTs) has attracted much research interest in view of their superior characteristics and novel properties induced by the interaction between them.<sup>1</sup> For example, inorganic semiconductor NPs such as TiO<sub>2</sub> and ZnO attached on CNTs with high conductivity demonstrated remarkably enhanced photoelectric and photocatalytic properties.<sup>2</sup> CNTs with large surface areas are ideal support to promote catalyst efficiency. Unfortunately, uniform performance was hampered by the difficulty of uniform attachment of metal or oxide NPs on the chemically inert CNTs, especially in the case of metal oxide.<sup>1</sup> The quality of the metal-oxide NPs/CNTs fabricated by conventional NP-synthesizing methods is far from the desired.<sup>3a</sup> Although layer-by-layer assembly using preformed NPs as building blocks on CNTs has successfully fabricated high-quality metal oxide NPs/CNTs,<sup>3b</sup> the cost and mass production remain unresolved. Therefore, developing a more facile, large-scale, and low-cost route to synthesize uniform metal oxide NPs/CNTs composites is of interest from fundamental research to their applications.

Solvothermal method is versatile for developing controlled assembly of NPs on CNT templates.<sup>4</sup> Surfactants are often used for improving the interface between NPs and the CNTs. However, size control and aggregation prevention during the assembly receive no deserved attention. Using a bifunctional surfactant that can also cap NPs for acquiring unified size, shape, and monodispersity might simplify the assembly mechanism with CNTs and thus improve the loading efficiency and homogeneity. With this in mind, in a solvothermal (*N,N*-dimethylformamide, DMF) system, we selected bifunctional phenol as surfactant to attach CNT via  $\pi$ - $\pi$  interaction between the delocalized  $\pi$ -electrons system of CNTs and the aromatic ending. It spontaneously capped the solvothermally grown iron oxides NPs via hydroxy groups for size control and aggregation inhibition, thus large-scale, uniform iron oxide NPs on single- or multiwalled CNTs (SWCNTs, MWCNTs) were achieved. With careful characterization including transmission electronic microscopy (TEM), high-resolution (HR)-TEM, and Raman spectroscopy, the magnetic properties of the composites are concisely discussed.

The experimental details and some of additional data are provided in the Electronic Supporting Information (ESI).<sup>11</sup> Based on the X-ray diffraction (XRD) analysis (ESI, Figure S1<sup>11</sup>), the presence of phenol greatly affected the size and phase of solution-formed iron oxides, which were indexed to be magnetic  $\gamma$ -Fe<sub>2</sub>O<sub>3</sub> rather than  $\alpha$ -Fe<sub>2</sub>O<sub>3</sub>, with a much smaller size (<5 nm). The

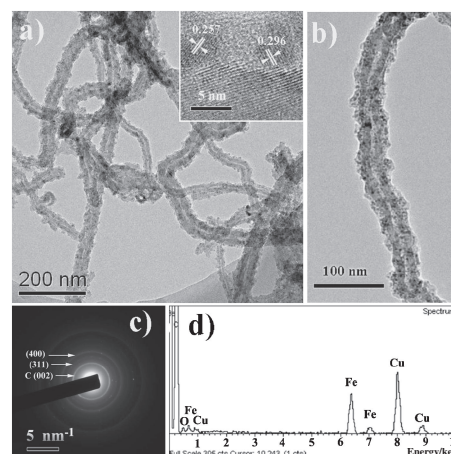


**Figure 1.** (a), (b): Representative TEM images of the  $\gamma$ -Fe<sub>2</sub>O<sub>3</sub>/MWCNT nanohybrids. Inset (a) shows the HR-TEM image. (c) and (d) indicate the selected-area electron diffraction (SAED) pattern and energy-dispersive spectrum (EDS), respectively.

attached  $\gamma$ -Fe<sub>2</sub>O<sub>3</sub> NPs on MWCNTs and SWCNTs were denoted as  $\gamma$ -Fe<sub>2</sub>O<sub>3</sub>/MWCNTs and  $\gamma$ -Fe<sub>2</sub>O<sub>3</sub>/SWCNTs, respectively. The unattached  $\gamma$ - and  $\alpha$ -Fe<sub>2</sub>O<sub>3</sub> NPs were also prepared. Figures 1a and 1b display the TEM images of the  $\gamma$ -Fe<sub>2</sub>O<sub>3</sub>/MWCNTs and the singular tube. From Figure 1a, the carbon nanotubes interlaced each other with a rough surface, unlike the smooth surface of MWCNTs (ESI, Figure S2<sup>11</sup>), implying the uniform attachment of  $\gamma$ -Fe<sub>2</sub>O<sub>3</sub> NPs on the MWCNTs. No  $\gamma$ -Fe<sub>2</sub>O<sub>3</sub> NPs with large grain size on the MWCNT were observed, quite different from the case fabricated by traditional method.<sup>3a</sup> From the HR-TEM image in the inset, the  $\gamma$ -Fe<sub>2</sub>O<sub>3</sub> NPs with defined structures and small dimension were anchored on MWCNTs, greatly different from the coarse  $\alpha$ -Fe<sub>2</sub>O<sub>3</sub> (ESI, Figure S3<sup>11</sup>). From the lattice fringes, the two adjacent plane distances are about 0.257 and 0.296 nm, corresponding to the interlayer spacing of the (311) and (220) planes of the  $\gamma$ -Fe<sub>2</sub>O<sub>3</sub>, respectively.<sup>5</sup> From the SAED pattern in Figure 1c, the rings corresponding to the (002) plane of graphite and the (311) and (400) planes of  $\gamma$ -Fe<sub>2</sub>O<sub>3</sub> were observed. The latter two indicate the polycrystalline characteristic of the  $\gamma$ -Fe<sub>2</sub>O<sub>3</sub>. The EDS pattern in Figure 1d confirmed that the main element components are carbon and iron.

The loading density of the  $\gamma$ -Fe<sub>2</sub>O<sub>3</sub> on MWCNTs can be facilely tuned by varying the input mass ratio of raw materials. Figure 2 shows the TEM images of  $\gamma$ -Fe<sub>2</sub>O<sub>3</sub>/MWCNTs (a, b) and the  $\gamma$ -Fe<sub>2</sub>O<sub>3</sub>/SWCNTs composites (d) with an input mass ratio of Fe(NO<sub>3</sub>)<sub>3</sub>/C = 9. It clearly shows that highly loaded  $\gamma$ -Fe<sub>2</sub>O<sub>3</sub> NPs were homogeneously assembled on the CNTs, with size almost unchanged. The content of oxides in the composites can be tuned from 16 to 40 wt % by increasing the input mass ratio of Fe(NO<sub>3</sub>)<sub>3</sub>/C from 1:1 to 9:1, determined from TG analysis (Figure 2c).

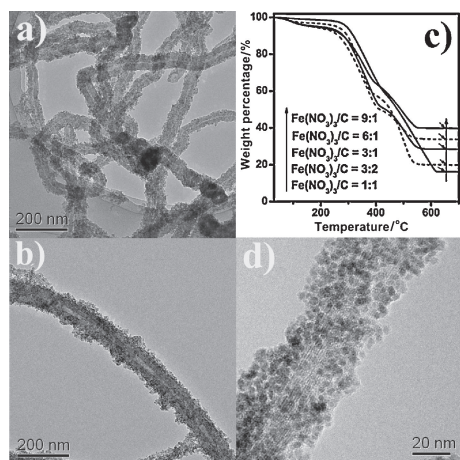


**Figure 2.** TEM images of  $\gamma$ -Fe<sub>2</sub>O<sub>3</sub>/MWCNTs (a, b) and  $\gamma$ -Fe<sub>2</sub>O<sub>3</sub>/SWCNTs nanocomposites (d) prepared with a input mass ratio of Fe(NO<sub>3</sub>)<sub>3</sub>/C = 9. (c) shows the TGA data of  $\gamma$ -Fe<sub>2</sub>O<sub>3</sub>/MWCNTs with different loading.

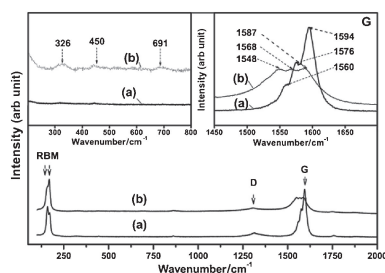


**Figure 3.** Raman spectra of (a) the pristine SWCNTs and (b) the  $\gamma$ -Fe<sub>2</sub>O<sub>3</sub>/SWCNTs (Fe<sub>2</sub>O<sub>3</sub>% = 30 wt %) in full range of 100–2000 cm<sup>-1</sup>. Left inset displays the detailed Raman spectra in the 200–800 cm<sup>-1</sup> spectral range, and right inset is the enlarged G band.

Raman spectroscopy was used to check the interfacial interaction between CNTs and the iron oxides. The  $\gamma$ -Fe<sub>2</sub>O<sub>3</sub>/SWCNTs (Fe<sub>2</sub>O<sub>3</sub>% = 30 wt %) was used as model sample since SWCNTs are sensitive to the charge interaction with guest compounds.<sup>6</sup> Figure 3 displays the Raman spectra of SWCNTs and the  $\gamma$ -Fe<sub>2</sub>O<sub>3</sub>/SWCNTs irradiated at 785 nm. In full spectra, the representative Raman peaks of SWCNTs including the tangential (G) band ranging from 1450 to 1650 cm<sup>-1</sup> are visible, as are enlarged in the right inset. It is clear that the G band of  $\gamma$ -Fe<sub>2</sub>O<sub>3</sub>/SWCNTs with three peaks downshifted from primarily about 1560, 1576, and 1594 cm<sup>-1</sup> to about 1548, 1568, and 1587 cm<sup>-1</sup>, respectively, indicating the n-doping of SWCNTs<sup>7</sup> and the interfacial electron transfer is from iron oxide to CNTs. In addition, several broad and not well-defined peaks at about 326, 450, and 691 cm<sup>-1</sup> are uniquely attributed to  $\gamma$ -Fe<sub>2</sub>O<sub>3</sub> (Figure 3, left inset).<sup>7</sup>

The decoration of CNTs with various structural and dimensional iron oxides could increase the tunability of their magnetic and electric properties.<sup>8</sup> Figure 4 presents the magnetization curves of the  $\gamma$ -Fe<sub>2</sub>O<sub>3</sub>/MWCNTs (Fe<sub>2</sub>O<sub>3</sub>% = 28 wt %) in comparison with those of the unattached  $\gamma$ -Fe<sub>2</sub>O<sub>3</sub> and MWCNTs at 2 K and room temperature (300 K). MWCNTs appear diamagnetic, while the  $\gamma$ -Fe<sub>2</sub>O<sub>3</sub> NPs appear superparamagnetic at room temperature, due to the finite size effect.<sup>9</sup> Differing from the unattached  $\gamma$ -Fe<sub>2</sub>O<sub>3</sub>, the  $\gamma$ -Fe<sub>2</sub>O<sub>3</sub>/MWCNTs demonstrates weak ferromagnetism at room temperature. No saturated magnetization appears even under an

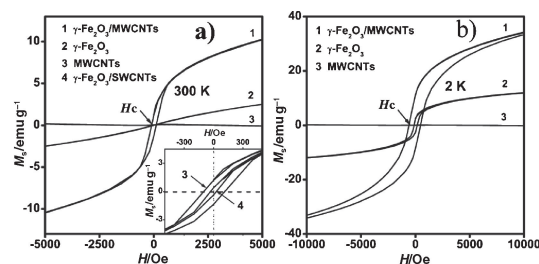


**Figure 4.** Hysteresis loops of the  $\gamma$ -Fe<sub>2</sub>O<sub>3</sub>/MWCNTs composite (Fe<sub>2</sub>O<sub>3</sub>% = 28 wt %),  $\gamma$ -Fe<sub>2</sub>O<sub>3</sub>, and MWCNTs measured at (a) 300 and (b) 2 K. Inset shows the enlarged magnetization of the  $\gamma$ -Fe<sub>2</sub>O<sub>3</sub>/SWCNTs (Fe<sub>2</sub>O<sub>3</sub>% = 30 wt %) including the  $\gamma$ -Fe<sub>2</sub>O<sub>3</sub>/MWCNTs composites.

external magnetic field of 8 T. The coercivity ( $H_c$ ) at 300 K is 112 Oe, much larger than that of bulk iron (1 Oe).<sup>9</sup> At 2 K, they present enhanced ferromagnetism because of the increased magnetic anisotropy at low temperature. The magnetic variation between the unattached  $\gamma$ -Fe<sub>2</sub>O<sub>3</sub> and the  $\gamma$ -Fe<sub>2</sub>O<sub>3</sub>/MWCNTs can be explained from the interfacial interaction of their two components. From the Raman feature of the  $\gamma$ -Fe<sub>2</sub>O<sub>3</sub>/SWCNTs, the downshifts of the G band suggest the electron transfer from the iron oxides to CNTs, producing positively charged holes. The separated holes might be captured by the cation vacancies or defects present in nano  $\gamma$ -Fe<sub>2</sub>O<sub>3</sub>.<sup>10a</sup> The magnetic exchange interactions between the high-spin state charged vacancies give rise to ferromagnetism. Moreover, the captured hole may also promote the atomic magnetic coupling of electronic spins of the next-nearest neighbor Fe<sup>3+</sup> in the crystal structure,<sup>10b</sup> thus increasing the magnetic anisotropy of iron oxides. Similar phenomenon was observed in the  $\gamma$ -Fe<sub>2</sub>O<sub>3</sub>/SWCNTs (inset, curve 4).

In summary, a developed solvothermal method can facilely synthesize uniform  $\gamma$ -Fe<sub>2</sub>O<sub>3</sub> NPs/CNTs composite by using a bifunctional surfactant. This approach can easily be extended to other metal oxides–CNTs composites.

This work was financially supported by the National Key Project on Basic Research (Grant No. 2009CB939801), the Natural Science Foundation of Fujian Province (Grant No. 2009J01044), and Fujian Institute of Research on the Structure of Matter (Grant No. SZD09003), Chinese Academy of Sciences (CAS).

#### References and Notes

- 1 a) X. Peng, J. Chen, J. A. Misewich, S. S. Wong, *Chem. Soc. Rev.* **2009**, *38*, 1076, and the references there in. b) H. Chu, L. Wei, R. Cui, J. Wang, Y. Li, *Coord. Chem. Rev.* **2010**, *254*, 1117, and the references there in.
- 2 K. Woan, G. Pyrgiotakis, W. Sigmund, *Adv. Mater.* **2009**, *21*, 2233.
- 3 a) W.-Q. Han, A. Zettl, *Nano Lett.* **2003**, *3*, 681. b) J. Li, S. Tang, L. Lu, H. C. Zeng, *J. Am. Chem. Soc.* **2007**, *129*, 9401.
- 4 Y. J. Na, H. S. Kim, J. Park, *J. Phys. Chem. C* **2008**, *112*, 11218.
- 5 J. Wang, Y. Ma, K. Watanabe, *Chem. Mater.* **2008**, *20*, 20.
- 6 M. S. Dresselhaus, G. Dresselhaus, R. Saito, A. Jorio, *Phys. Rep.* **2005**, *409*, 47.
- 7 D. L. A. de Faria, S. V. Silva, M. T. de Oliveira, *J. Raman Spectrosc.* **1997**, *28*, 873.
- 8 G. Korneva, H. Ye, Y. Gogotsi, D. Halverson, G. Friedman, J.-C. Bradley, K. G. Kornev, *Nano Lett.* **2005**, *5*, 879.
- 9 D. Li, W. Y. Teoh, C. Selomulya, R. C. Woodward, P. Munroe, R. Amal, *J. Mater. Chem.* **2007**, *17*, 4876.
- 10 a) A. Sundaresan, C. N. R. Rao, *Solid State Commun.* **2009**, *149*, 1197, and the references there in. b) X. Qiu, L. Li, C. Tang, G. Li, *J. Am. Chem. Soc.* **2007**, *129*, 11908.
- 11 Supporting Information is available electronically on the CSJ-Journal Web site, <http://www.csj.jp/journals/chem-lett/index.html>.